

Classification

Physics Abstracts

03.65 — 32.80 — 42.50 — 42.69

Coherent population trapping and Fano profiles

B. Lounis and C. Cohen-Tannoudji

Laboratoire de Spectroscopie Hertzienne de l'E.N.S.(*) and Collège de France, 24 rue Lhomond, F-75231 Paris Cedex 05, France

(Received 15 January 1992, accepted 23 January 1992)

Résumé . — Cet article présente une nouvelle approche au phénomène de piégeage cohérent de population observable sur un système atomique à 3 niveaux en configuration Λ . Cette approche, basée sur la théorie de la diffusion, est valable lorsqu'un des deux champs lasers excitant le système atomique est beaucoup plus faible que l'autre. L'amplitude de diffusion du champ faible apparaît comme la somme de deux amplitudes résonnantes. Les positions et les largeurs des deux résonances correspondantes sont calculées et interprétées physiquement, à la limite des faibles saturations, en termes de diffusion Rayleigh et de diffusion Raman stimulée et spontanée. On montre enfin que l'interférence entre ces deux amplitudes de diffusion fait apparaître des profils de Fano dans les courbes donnant les variations en fréquence de la section efficace totale de diffusion.

Abstract . — This paper presents a new approach to coherent population trapping in a Λ -type three level atomic configuration. This approach, which is based on scattering theory, applies when one of the two driving laser fields is much weaker than the other one. We show that the scattering amplitude of the weak field is the sum of 2 resonant amplitudes. The positions and the widths of these resonances are identified and physically interpreted in the low saturation limit, in terms of Rayleigh scattering, stimulated and spontaneous Raman scattering. Finally, we show that the interference between the two scattering amplitudes gives rise to Fano profiles in the curves giving the frequency dependence of the total scattering cross-section.

1. Introduction.

We consider in this paper an atomic system with three levels, e, g_1, g_2 , forming a Λ -configuration (Fig. 1). The two transitions $g_1 - e$ and $g_2 - e$ are driven by two laser fields with frequencies ω_{L1} and ω_{L2} close, respectively, to the atomic frequencies $\omega_{e1} = (E_e - E_{g1})/\hbar$ and $\omega_{e2} = (E_e - E_{g2})/\hbar$. We denote :

(*) Laboratoire associé au C.N.R.S. et à l'Université Pierre et Marie Curie.

$$\delta_1 = \omega_{L1} - \omega_{e1} \quad \delta_2 = \omega_{L2} - \omega_{e2} \quad (1.1)$$

the corresponding detunings between the laser and atomic frequencies. The atom can decay from e to g_1 and from e to g_2 by spontaneous emission with rates respectively equal to Γ_1 and Γ_2 . We put :

$$\Gamma = \Gamma_1 + \Gamma_2 \quad (1.2)$$

We assume that g_2 is above g_1 ($E_{g_2} > E_{g_1}$), but that no spontaneous emission can occur from g_2 to g_1 .

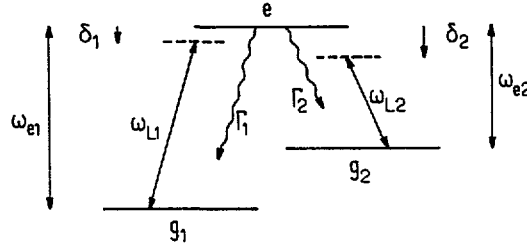


Fig. 1. — Three level Λ -configuration $\{e, g_1, g_2\}$ driven by two laser fields at frequencies ω_{L1} and ω_{L2} . $\delta_1 = \omega_{L1} - \omega_{e1}$ and $\delta_2 = \omega_{L2} - \omega_{e2}$ are the two detunings; Γ_1 and Γ_2 are, respectively, the two spontaneous emission rates from e to g_1 and g_2 .

Such a configuration gives rise to the phenomenon of “coherent population trapping” [1, 2]. When the two detunings δ_1 and δ_2 are equal, i.e. when the resonance Raman condition :

$$\hbar\omega_{L1} - \hbar\omega_{L2} = E_{g_2} - E_{g_1} \quad (1.3)$$

between the two states g_1 and g_2 is fulfilled, the steady-state population σ_{ee}^{st} of the upper state vanishes and the fluorescence stops. Several theoretical treatments have been given for such an effect [3-6]. The main result is that atoms are optically pumped in a linear superposition of the two lower states which is not coupled to the laser light because the two absorption amplitudes from g_1 to e and from g_2 to e interfere destructively. Several applications of coherent population trapping have been developed, including high resolution spectroscopy [7], subrecoil laser cooling [8], adiabatic transfer of populations [9], amplification without inversion [10].

Suppose that ω_{L2} is fixed and that ω_{L1} is scanned. The variations with ω_{L1} , or equivalently with $\delta_1 = \omega_{L1} - \omega_{e1}$, of σ_{ee}^{st} may be studied from the steady-state solution of optical Bloch equations, which can be determined analytically and which may be found for example in reference [5].

$$\sigma_{ee}^{st} = \frac{4(\delta_1 - \delta_2)^2 \Omega_1^2 \Omega_2^2 \Gamma}{Z} \quad (1.4)$$

where

$$\begin{aligned} Z = & 8(\delta_1 - \delta_2)^2 \Omega_1^2 \Omega_2^2 \Gamma + 4(\delta_1 - \delta_2)^2 \Gamma^2 (\Omega_1^2 \Gamma_2 + \Omega_2^2 \Gamma_1) \\ & + 16(\delta_1 - \delta_2)^2 [\delta_1^2 \Omega_2^2 \Gamma_1 + \delta_2^2 \Omega_1^2 \Gamma_2] - 8\delta_1(\delta_1 - \delta_2) \Omega_2^4 \Gamma_1 \\ & + 8\delta_2(\delta_1 - \delta_2) \Omega_1^4 \Gamma_2 + (\Omega_1^2 + \Omega_2^2)^2 (\Omega_1^2 \Gamma_2 + \Omega_2^2 \Gamma_1) \end{aligned} \quad (1.5)$$

In (1.4) and (1.5), Ω_1 and Ω_2 are the Rabi frequencies characterizing, respectively, the couplings of the two laser fields at ω_{L1} and ω_{L2} with the transitions $g_1 - e$ and $g_2 - e$. The variations with

δ_1 of σ_{ee}^{st} are represented in figure 2, in the limiting case where $\Omega_2 \gg \Omega_1$. We have supposed $\delta_2 = -1.5\Gamma$. They clearly exhibit two resonances : a broad one, near $\delta_1 = 0$, and a narrow one near $\delta_1 = \delta_2$, where σ_{ee}^{st} vanishes. The narrow structure of figure 2 is quite similar to the Fano profiles which can be observed when a discrete state is coupled to a continuum via two channels, directly and through a discrete state embedded in this continuum [11]. Well known examples of such profiles are found in autoionizing resonances [11] and in laser induced continuum structures [12 - 13].

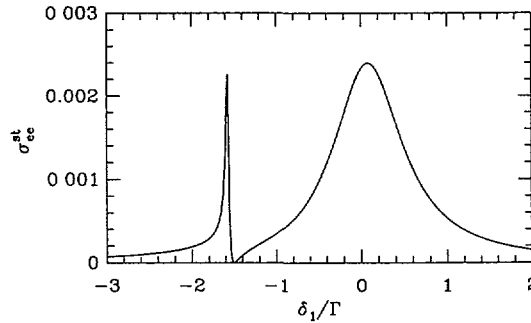


Fig. 2. — Steady-state population of the excited state, calculated from optical Bloch equations, versus δ_1 in units of Γ . δ_2 is fixed and equal to -1.5Γ , $\Omega_2 = 0.7\Gamma$, $\Omega_1 = 0.025\Gamma$. Two resonances are clearly visible, the narrow one looking like a Fano profile.

The purpose of this paper is to investigate the connections which exist between coherent population trapping in a Λ -configuration and Fano profiles. Such a connection cannot be easily analyzed from expressions such as (1.4) and (1.5) which have not a transparent physical meaning. We prefer to adopt here another point of view which, we hope, can provide new physical insights in coherent population trapping. We consider the scattering of a single photon ω_{L1} by the atom interacting with several ω_{L2} photons and we try to identify in the total scattering amplitude the various physical paths followed by the system and whose interference can give rise to structures such as the one appearing in figure 2. The paper is organized as follows. We first specify in section 2 our assumptions on the scattering process considered in this paper. A non-perturbative expression for the scattering amplitude is then derived in section 3 and its general properties are analyzed. The limiting case where the transition $g_2 - e$ is not saturated by the ω_{L2} photons is investigated in section 4 and this allows us to identify the physical processes associated with the two resonances of figure 2. Finally, we show in section 5 how Fano profiles can be associated with the narrow structure of figure 2.

2. Scattering process considered in this paper.

2.1 INITIAL STATE AND FINAL STATE. — In the initial state :

$$|i\rangle = |g_1; (1)_1, (N)_2, (0)_j\rangle \quad (2.1)$$

of the scattering process, the atom is in g_1 , in the presence of 1 photon ω_{L1} , N photons ω_{L2} , all other field modes j (with $j \neq 1, 2$) being empty. We consider here the scattering process

leading to the final state :

$$|f\rangle = |g_1; (0)_1, (N)_2, (1)_\omega\rangle \quad (2.2)$$

where the atom is still in g_1 , whereas the incident photon ω_{L1} has disappeared and has been replaced by one fluorescence photon ω .

The final state (2.2) is not the only possible one. Other scattering processes, involving several fluorescence photons and the absorption of one or several ω_{L2} photons could also be considered. For each of these possible scattering processes, starting from (2.1), the atom has first to go from g_1 to e , and one can show that the total cross-section for each of these scattering processes is proportional to the steady-state population of e . Since we are mainly interested here in σ_{ee}^{st} , we restrict ourselves to the simplest possible scattering process, the one leading from (2.1) to (2.2). We will check in subsection 3.4 that the total scattering cross section for such a process is proportional to σ_{ee}^{st} . Note also that g_2 cannot appear in the final state of a scattering process. Photons ω_{L2} can indeed be absorbed by the atom in g_2 , so that g_2 is an unstable state.

When the radiation field is quantized in a box of volume L^3 , the Rabi frequencies Ω_1 and Ω_2 associated with (2.1) are respectively proportional to :

$$\Omega_1 \sim \sqrt{\frac{\hbar\omega_{L1}}{2\varepsilon_0 L^3}} \quad \Omega_2 \sim \sqrt{\frac{N\hbar\omega_{L2}}{2\varepsilon_0 L^3}} \quad (2.3)$$

The fact that Ω_1 tends to zero when $L \rightarrow \infty$ does not raise any difficulty. The flux associated with the incident photon ω_{L1} is equal to c/L^3 and the ratio of the transition rate, proportional to Ω_1^2 , i.e. to $1/L^3$, by the incident flux c/L^3 , is independent of L , as expected for a physical quantity such as a scattering cross section. The situation is different for Ω_2 . When L tends to infinity, we must also let N tend to infinity, keeping N/L^3 constant, in order to have Ω_2 fixed.

2.2 ASSUMPTIONS CONCERNING THE INTERACTION HAMILTONIAN V. — The Hamiltonian H of the total system "atom + photons" is equal to :

$$H = H_0 + V \quad (2.4)$$

where V is the photon-atom interaction Hamiltonian and where H_0 is the sum of the energies of the non interacting systems.

In the electric-dipole and rotating-wave approximations, V can be written :

$$V = -\mathbf{d}^+ \cdot \mathbf{E}^+ - \mathbf{d}^- \cdot \mathbf{E}^- \quad (2.5)$$

where \mathbf{d}^+ and \mathbf{d}^- are, respectively, the raising and lowering parts of the dipole operator, and where \mathbf{E}^+ and \mathbf{E}^- are, respectively, the positive and negative frequency components of the electric field operator. With such an interaction Hamiltonian, the only processes which can take place when the atom is in g_1 , is the absorption of one photon, the atom going from g_1 to e . We make here the further assumption that ω_{e1} and ω_{e2} are so different that it is legitimate to neglect the non resonant coupling of photons ω_{L2} with the atom in g_1 .

From the previous assumptions, it follows that V acting upon $|i\rangle$ can lead only to $|e; (0)_1, (N)_2, (0)_j\rangle$. More precisely,

$$V|i\rangle = \frac{\hbar\Omega_1}{2} |e; (0)_1, (N)_2, (0)_j\rangle \quad (2.6)$$

which is the precise definition of the Rabi frequency Ω_1 . Similarly,

$$V|f\rangle = \frac{\hbar\Omega}{2} |e; (0)_1, (N)_2, (0)_j\rangle \quad (2.7)$$

where Ω is the Rabi frequency characterizing the coupling with the fluorescence photon ω .

3. Calculation of the scattering amplitude.

3.1 GENERAL EXPRESSION OF THE S -MATRIX ELEMENT. — Since we neglect virtual emissions of photons by the atom in g_1 (rotating-wave approximation), the states $|i\rangle$ and $|f\rangle$ introduced above can be considered as correct asymptotic scattering states (see for example, Ref. [14], Complement B_{III}). The element $S_{\bar{n}}$ of the S -matrix, between the initial and final states, can then be written :

$$S_{\bar{n}} = \delta_{\bar{n}} - 2\pi i \delta(E_f - E_i) T_{\bar{n}} \quad (3.1)$$

where E_i and E_f are the unperturbed energies of $|i\rangle$ and $|f\rangle$ (which are eigenstates of H_0), and where the transition matrix element $T_{\bar{n}}$ is given by :

$$T_{\bar{n}} = \langle f | V | i \rangle + \lim_{\eta \rightarrow 0^+} \left\langle f \left| V \frac{1}{E_i - H + i\eta} V \right| i \right\rangle \quad (3.2)$$

Note that it is H , and not H_0 , which appears in the exact expression (3.2). Expanding the propagator $(E_i - H + i\eta)^{-1}$ in powers of the unperturbed propagator $(E_i - H_0 + i\eta)^{-1}$ and V would give the Born expansion of the scattering matrix. We don't make such an expansion here. We keep the exact expression (3.2), in order to get non perturbative scattering amplitudes including the shift and the broadening of the intermediate states appearing in the scattering process.

3.2 CONNECTION BETWEEN THE SCATTERING-MATRIX AND THE RESOLVENT $G(z)$ OF THE HAMILTONIAN. — In order to connect $|i\rangle$ to $|f\rangle$, one must destroy the incident photon ω_{L1} and create the scattered photon ω . The interaction Hamiltonian V , given in (2.5), can only destroy or create a single photon at a time. It follows that :

$$\langle f | V | i \rangle = 0 \quad (3.3)$$

Using (2.6) and (2.7), we can then transform (3.2) into :

$$T_{\bar{n}} = \frac{\hbar^2 \Omega \Omega_1}{4} \lim_{\eta \rightarrow 0^+} \langle \varphi_e | G(z = E_i + i\eta) | \varphi_e \rangle \quad (3.4)$$

where :

$$G(z) = \frac{1}{z - H} \quad (3.5)$$

is the resolvent of the Hamiltonian H , z being a complex variable, and where we have introduced the simplified notation :

$$|\varphi_e\rangle = |e; (0)_1, (N)_2, (0)_j\rangle \quad (3.6)$$

3.3 CALCULATION OF THE RELEVANT MATRIX ELEMENTS OF THE RESOLVENT. — The atom, in e , can spontaneously emit a photon and decay to g_1 or g_2 . The state $|\varphi_e\rangle$, given in (3.6), is thus coupled to continua and radiatively unstable. Well known projection operator techniques are available for calculating the diagonal element $G_{ee}(z) = \langle \varphi_e | G(z) | \varphi_e \rangle$ (see for example Ref. [14], Chap. III). Before doing such a calculation, one must not forget however to check if there are no other discrete states of H_0 , close to $|\varphi_e\rangle$, and which would be coupled to $|\varphi_e\rangle$ or to the same continua as $|\varphi_e\rangle$. In such a case, it is well known that the decay of $|\varphi_e\rangle$ cannot

be studied independently of these other discrete states. Simple expressions for the matrix elements of $G(z)$ can be obtained only if one considers the projection of $G(z)$ onto the subspace \mathcal{E}_0 subtended by the discrete states of H_0 which are coupled directly or indirectly through the same continua.

Actually, in the problem considered in this paper, we have another discrete state of H_0

$$|\varphi_2\rangle = |g_2; (0)_1, (N+1)_2, (0)_j\rangle \quad (3.7)$$

which is coupled to $|\varphi_e\rangle$ since the atom in g_2 can absorb one ω_{L2} photon and jump to e . By definition of the Rabi frequency Ω_2 , we have indeed :

$$\langle \varphi_e | V | \varphi_2 \rangle = \langle e; (0)_1, (N)_2, (0)_j | V | g_2; (0)_1, (N+1)_2, (0)_j \rangle = \frac{\hbar\Omega_2}{2} \quad (3.8)$$

Furthermore, the unperturbed energies E_{φ_e} and E_{φ_2} of $|\varphi_e\rangle$ and $|\varphi_2\rangle$ are close to each other. If we measure the unperturbed energies relative to E_{φ_e} , by taking :

$$E_{\varphi_e} = 0 \quad (3.9)$$

then, we have :

$$E_{\varphi_2} = \hbar\delta_2 \quad (3.10)$$

Strictly speaking, one should also consider the initial state $|i\rangle$ given in (2.1), which is coupled to $|\varphi_e\rangle$, since, according to (2.6),

$$\langle \varphi_e | V | i \rangle = \frac{\hbar\Omega_1}{2} \quad (3.11)$$

This state has an energy E_i close to $E_{\varphi_e} = 0$

$$E_i = \hbar\delta_1 \quad (3.12)$$

One must not forget however that, in the limit $L \rightarrow \infty$, Ω_1 tends to zero (whereas Ω_2 keeps the same value), so that we can neglect the influence of $|i\rangle$ on the decay of $|\varphi_e\rangle$.

The previous discussion shows that we must introduce a two dimensional subspace \mathcal{E}_0 of eigenstates of H_0

$$\mathcal{E}_0 = \{|\varphi_e\rangle, |\varphi_2\rangle\} \quad (3.13)$$

and study $PG(z)P$, where P is the projector onto this subspace. One can then show (see, for example, Ref. [14], Chap. III) that, when z is close to $E_i + i\eta$, $PG(z)P$ can be considered as the resolvent of an effective Hamiltonian H_{eff}

$$PG(z)P = \frac{P}{z - H_{\text{eff}}} \quad (3.14)$$

Such a Hamiltonian governs the evolution of the system within \mathcal{E}_0 and is represented by the following 2×2 matrix :

$$(H_{\text{eff}}) = \hbar \begin{pmatrix} -i\Gamma/2 & \Omega_2/2 \\ \Omega_2/2 & \delta_2 \end{pmatrix} \quad (3.15)$$

Note that H_{eff} differs from $PH_0P + PVP$ only by an imaginary term, $-i\hbar\Gamma/2$, added to the energy of the excited state e , and describing the radiative unstability of this state.

Written in matrix form, the operator equation (3.14) becomes for $z = E_i + i\eta = \hbar\delta_1 + i\eta$, according to (3.12) :

$$\begin{pmatrix} G_{ee}(\hbar\delta_1 + i\eta) & G_{2e}(\hbar\delta_1 + i\eta) \\ G_{e2}(\hbar\delta_1 + i\eta) & G_{ee}(\hbar\delta_1 + i\eta) \end{pmatrix} = \frac{1}{\hbar} \begin{pmatrix} \delta_1 + i\frac{\Gamma}{2} & -\frac{\Omega_2}{2} \\ -\frac{\Omega_2}{2} & \delta_1 - \delta_2 \end{pmatrix}^{-1} \quad (3.16)$$

Since the two eigenvalues of H_{eff} are complex, we have not kept $i\eta$ in the matrix appearing in right-hand side of (3.16). Taking the inverse of this matrix, and using (3.4) and (3.12), we get :

$$T_{\hbar} = \frac{\hbar\Omega_1\Omega}{4} \frac{\delta_1 - \delta_2}{\mathcal{D}} \quad (3.17)$$

where

$$\mathcal{D} = \left(\delta_1 + i\frac{\Gamma}{2} \right) (\delta_1 - \delta_2) - \frac{\Omega_2^2}{4} = \delta_1 (\delta_1 - \delta_2) - \frac{\Omega_2^2}{4} + i\frac{\Gamma}{2} (\delta_1 - \delta_2) \quad (3.18)$$

is the determinant of the matrix $\delta_1 - H_{\text{eff}}/\hbar$. Introducing the eigenvalues $\hbar z_I$ and $\hbar z_{II}$ of H_{eff} , we can also write :

$$\mathcal{D} = (\delta_1 - z_I)(\delta_1 - z_{II}) \quad (3.19)$$

which, inserted into (3.17), gives :

$$T_{\hbar} = \frac{\hbar\Omega_1\Omega}{4} \frac{\delta_1 - \delta_2}{(\delta_1 - z_I)(\delta_1 - z_{II})} = \frac{\hbar\Omega_1\Omega}{4(z_I - z_{II})} \left[\frac{z_I - \delta_2}{\delta_1 - z_I} - \frac{z_{II} - \delta_2}{\delta_1 - z_{II}} \right] \quad (3.20)$$

3.4 GENERAL PROPERTIES OF THE SCATTERING AMPLITUDE. — Considered as a function of δ_1 , the scattering amplitude T_{\hbar} appears in (3.20) as a sum of two resonant scattering amplitudes : one centered about $\delta_1 = \text{Re } z_I$, with a width equal to $\text{Im } z_I$; and the other one centered about $\delta_1 = \text{Re } z_{II}$, with a width equal to $\text{Im } z_{II}$. The theoretical approach followed in this paper clearly shows that two resonances should appear in the variation with δ_1 of the total scattering cross-section (which is proportional to $|T_{\hbar}|^2$), and it relates the positions and the widths of these resonances to the real and imaginary parts of the eigenvalues of H_{eff} .

It also clearly appears from (3.17) that T_{\hbar} vanishes for $\delta_1 = \delta_2$. The quenching of the fluorescence, when the resonance Raman condition between g_1 and g_2 is fulfilled, is also predicted by such an approach.

Let us finally calculate $|T_{\hbar}|^2$. Using (3.17) and (3.18), we get :

$$|T_{\hbar}|^2 = \frac{\hbar^2\Omega_1^2\Omega^2}{16} \frac{(\delta_1 - \delta_2)^2}{\left[\delta_1 (\delta_1 - \delta_2) - \frac{\Omega_2^2}{4} \right]^2 + \frac{\Gamma^2}{4} (\delta_1 - \delta_2)^2} \quad (3.21)$$

It is interesting now to compare (3.21) with the limit of (1.4) when $\Omega_2 \gg \Omega_1$. Since Ω_1^2 already appears in the numerator of (1.4), we can put $\Omega_1 = 0$ in Z . One can then easily check that $|T_{\hbar}|^2$ and σ_{ee}^{st} are proportional, and have therefore the same dependence in $\delta_1, \delta_2, \Omega_2$. As expected, we find that the total scattering cross-section, for the process $|i\rangle \rightarrow |f\rangle$ considered in this paper, involves the steady-state population of e . In the limit $\Omega_1 \ll \Omega_2$, we can therefore get new physical insights in equations (1.4) and (1.5), and in the variations with δ_1 of σ_{ee}^{st} represented in figure 2, by considering the two resonant scattering amplitudes appearing in (3.20).

4. The low saturation limit. Physical discussion.

The calculations of the previous section 3 are valid for any value of Ω_2 and δ_2 . We consider now the limit where Ω_2 is small compared to Γ or to $|\delta_2|$. More precisely, we suppose that the saturation parameter s_2 for the transition $g_2 - e$ is small compared to 1 :

$$s_2 = \frac{\Omega_2^2/2}{\delta_2^2 + \frac{\Gamma^2}{4}} \ll 1 \quad (4.1)$$

Such a limit is interesting because it leads to two eigenvalues of H_{eff} , z_I and z_{II} , having quite different imaginary parts. The corresponding resonances appearing in the variations of $T_{\bar{n}}$ with δ_1 have then quite different widths, which is indeed the situation leading to Fano profiles.

4.1 INTERPRETATION OF THE TWO RESONANCES APPEARING IN THE SCATTERING AMPLITUDE. — Let z_{II} be the eigenvalue of H_{eff}/\hbar which tends to δ_2 when Ω_2 tends to zero. One can always write :

$$z_{II} = \delta_2 + \delta'_2 - i\frac{\Gamma'_2}{2} \quad (4.2)$$

where δ'_2 and $-i\Gamma'_2/2$ are the real and imaginary parts of the correction introduced by Ω_2 . Because the trace of H_{eff} is invariant in a change of basis, we have for the other eigenvalue z_I , which tends to $-i\Gamma/2$ when Ω_1 tends to zero :

$$z_I = -\delta'_2 - i\frac{\Gamma - \Gamma'_2}{2} \quad (4.3)$$

Condition (4.1) allows one to calculate δ'_2 and Γ'_2 perturbatively. One gets :

$$\delta'_2 - i\frac{\Gamma'_2}{2} = \frac{(\Omega_2/2)^2}{\delta_2 + i\frac{\Gamma}{2}} \quad (4.4)$$

which gives :

$$\delta'_2 = \delta_2 \frac{s_2}{2} \quad (4.5a)$$

$$\Gamma'_2 = \Gamma \frac{s_2}{2} \quad (4.5b)$$

Equation (4.5a) shows that δ'_2 is the light shift of level g_2 due to the coupling with the photons ω_{L2} , whereas equation (4.5b) shows that Γ'_2 is the radiative broadening of level g_2 , or equivalently the departure rate from level g_2 , due to the absorption of ω_{L2} photons. Note that, although δ'_2 and Γ'_2 are calculated here perturbatively, their presence in the denominator of the two fractions of (3.20) corresponds to a nonperturbative expression for $T_{\bar{n}}$. Finally, equation (4.3) shows that the light shift of level e is opposite to that of level g_2 , whereas the radiative width of level e is slightly reduced from Γ to $\Gamma - \Gamma'_2$ as a result of the contamination of e by g_2 induced by Ω_2 .

The physical meaning of δ'_2 and Γ'_2 can now be used to interpret the two resonances appearing in (3.22). Consider first the resonance associated with the denominator $\delta_1 - z_I$. The position of its center is given by :

$$\delta_1 = \text{Re } z_I = -\delta'_2 \quad (4.6)$$

an equation which can be also written :

$$\hbar\omega_{L1} = E_e - \hbar\delta'_2 - E_{g_1} \quad (4.7)$$

and which expresses an optical resonance condition between the lower level g_1 and the light-shifted upper level e . As expected, the width of this optical resonance, $\text{Im } z_1 = (\Gamma - \Gamma')/2 \simeq \Gamma/2$, is mainly determined by the natural width Γ of e . Consider now the second resonance associated with the denominator $\delta_1 - z_{\text{II}}$. Its position is determined by :

$$\delta_1 = \text{Re } z_{\text{II}} = \delta_2 + \delta'_2 \quad (4.8)$$

and corresponds to :

$$\hbar\omega_{L1} - \hbar\omega_{L2} = E_{g_2} + \hbar\delta'_2 - E_{g_1} \quad (4.9)$$

Equation (4.9) expresses a stimulated Raman resonance condition between the light-shifted level g_2 and the level g_1 . Note the difference between (4.9) and (1.3), which is the stimulated Raman resonance condition between unperturbed energy levels (without light shifts) leading to coherent population trapping. As for the width of the resonance associated with z_{II} , it is determined by the radiative width Γ'_2 of level g_2 due to the absorption of ω_{L2} photons. For small s_2 , this width is much smaller than Γ (see (4.5b)), so that the resonance associated with z_{II} is much narrower than the resonance associated with z_1 .

4.2 THE INTERMEDIATE STATES OF THE SCATTERING PROCESS. — From the results of subsection 3.2, it follows that the scattering amplitude T_{\hbar} can be written :

$$T_{\hbar} = \frac{\hbar^2 \Omega_1 \Omega}{4} \left\langle \overline{|\varphi_e\rangle} \left| \frac{1}{\hbar\delta_1 - H_{\text{eff}}} \right| \varphi_e \right\rangle \quad (4.10)$$

Let $\overline{|\varphi_e\rangle}$ and $\overline{|\varphi_2\rangle}$ be the eigenvectors of H_{eff} which tend to $|\varphi_e\rangle$ and $|\varphi_2\rangle$ when Ω_2 tends to zero. A perturbative expansion can be given for $\overline{|\varphi_e\rangle}$ and $\overline{|\varphi_2\rangle}$. Using (3.15), we get :

$$\overline{|\varphi_e\rangle} \simeq |\varphi_e\rangle - \frac{\Omega_2/2}{\delta_2 + i(\Gamma/2)} |\varphi_2\rangle \quad (4.11a)$$

$$\overline{|\varphi_2\rangle} \simeq |\varphi_2\rangle + \frac{\Omega_2/2}{\delta_2 + i(\Gamma/2)} |\varphi_e\rangle \quad (4.11b)$$

Note that $\overline{|\varphi_e\rangle}$ and $\overline{|\varphi_2\rangle}$ are not orthogonal, since H_{eff} is not hermitian. They form however a basis in the subspace \mathcal{E}_0 , and we can always expand $|\varphi_e\rangle$ on such a basis :

$$|\varphi_e\rangle = \alpha \overline{|\varphi_e\rangle} + \beta \overline{|\varphi_2\rangle} \quad (4.12)$$

the non orthogonality of $\overline{|\varphi_e\rangle}$ and $\overline{|\varphi_2\rangle}$ resulting in the fact that the components α and β of $|\varphi_e\rangle$ do not coincide respectively with the scalar products $\langle \overline{|\varphi_e\rangle} | \varphi_e \rangle$ and $\langle \overline{|\varphi_2\rangle} | \varphi_e \rangle$. Inserting (4.12) into (4.10) and using the fact that $\overline{|\varphi_e\rangle}$ and $\overline{|\varphi_2\rangle}$ are eigenstates of H_{eff} with eigenvalues $\hbar z_{\text{I}}$ and $\hbar z_{\text{II}}$, we get :

$$T_{\hbar} = \frac{\hbar \Omega_1 \Omega}{4} \left\{ \alpha \langle \overline{|\varphi_e\rangle} | \varphi_e \rangle \frac{1}{\delta_1 - z_{\text{I}}} + \beta \langle \overline{|\varphi_2\rangle} | \varphi_e \rangle \frac{1}{\delta_1 - z_{\text{II}}} \right\} \quad (4.13)$$

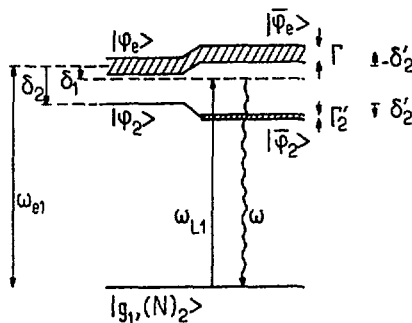


Fig. 3. — Diagrammatic representation of the scattering process in terms of dressed states. Starting from $|g_1, (N)_2\rangle$, the dressed atom absorbs the incident ω_{L1} photon (upward arrow), jumps to one of the two dressed states $|\overline{\varphi_e}\rangle$ or $|\overline{\varphi_2}\rangle$ originating from $|\varphi_e\rangle = |e, (N)_2\rangle$ and $|\varphi_2\rangle = |g_2, (N+1)_2\rangle$, and then falls back to $|g_1, (N)_2\rangle$ by emitting the fluorescence photon ω (downward wavy arrow).

Such a result shows that, after the absorption of the incident photon ω_{L1} , and before the emission of the fluorescence photon ω , the system passes through two possible intermediate states, which are the eigenstates $|\overline{\varphi_e}\rangle$ and $|\overline{\varphi_2}\rangle$ of H_{eff} .

These two states can be also considered as two dressed states of the "atom + ω_{L2} photons" system, as shown in figure 3. The left part of this figure represents a few unperturbed states of such a system : the two states $|\varphi_e\rangle = |e, (N)_2\rangle$ and $|\varphi_2\rangle = |g_2, (N+1)_2\rangle$, which are separated by an interval δ_2 (in angular frequency units), the state $|\varphi_e\rangle$ having a natural width Γ ; the state $|g_1, (N)_2\rangle$, which is located at a distance ω_{e1} below $|\varphi_2\rangle$. When the coupling $\Omega_2/2$ between $|\varphi_2\rangle$ and $|\varphi_e\rangle$ is taken into account, these two states repel each other by an amount δ'_2 , which is the light shift of g_2 , and transform into two dressed states $|\overline{\varphi_e}\rangle$ and $|\overline{\varphi_2}\rangle$ which are represented in the right part of figure 3. The contamination of the wave functions induced by Ω_2 is responsible for the appearance of a small width Γ'_2 for $|\overline{\varphi_2}\rangle$, whereas the width of $|\overline{\varphi_e}\rangle$ is slightly reduced. As for the state $|g_1, (N)_2\rangle$, it remains unperturbed, since we neglect the non resonant coupling of the atom in g_1 with the ω_{L2} photons. The scattering of the incident photon ω_{L1} by such a system can then be considered as an elastic scattering process, where the dressed atom, starting from $|g_1, (N)_2\rangle$, absorbs the incident photon ω_{L1} (upward arrow of Fig. 3), jumps to $|\overline{\varphi_2}\rangle$ or $|\overline{\varphi_e}\rangle$, and then falls back to $|g_1, (N)_2\rangle$ by emitting the fluorescence photon ω (downward wavy arrow). Another possible diagrammatic representation of such a process is given in figure 4, which represents more clearly than figure 3 the two possible intermediate states between the initial and final states. Note however that the energy defects in the two intermediate states are more visible on the diagrammatic representation of figure 3, where they are just equal to the interval between the dotted line (reached after the absorption of the ω_{L1} photon) and the energy of each dressed state $|\overline{\varphi_e}\rangle$ or $|\overline{\varphi_2}\rangle$, the width of each dressed state being included as an imaginary part of its energy.

The approach followed in this subsection could be easily extended to describe multiphoton scattering processes where several fluorescence photons are emitted and one or several ω_{L2} photons are absorbed. For example, the dressed atom in $|g_1, (N)_2\rangle$ can absorb the incident

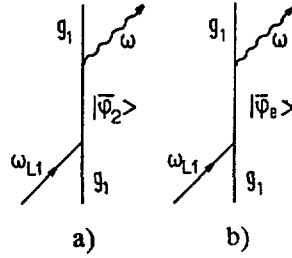


Fig. 4. — Another diagrammatic representation of the scattering process showing the two possible intermediate states $|\varphi_2\rangle$ and $|\varphi_e\rangle$.

photon ω_{L1} , jump to one of the two dressed states $|\varphi_e^N\rangle$ or $|\varphi_2^N\rangle$ originating from the manifold $\{|e, (N)_2\rangle, |g_2, (N+1)_2\rangle\}$, then emit a fluorescence photon ω' and fall into one of the two dressed states $|\varphi_e^{N-1}\rangle$ and $|\varphi_2^{N-1}\rangle$ originating from the manifold $\{|e, (N-1)_2\rangle, |g_2, (N)_2\rangle\}$, and finally end into $|g_1, (N-1)_2\rangle$ by emission of a second fluorescence photon ω'' . There are then four scattering amplitudes corresponding to four possible paths and one can show that, for $\delta_1 = \delta_2$, they interfere destructively two by two.

4.3 INTERPRETATION IN TERMS OF RAYLEIGH SCATTERING, STIMULATED AND SPONTANEOUS RAMAN SCATTERING. — When $\Omega_2 = 0$, the only scattering path which remains open is the one passing through $|\varphi_e\rangle = |e, (N)_2\rangle$ (Path b of Fig. 4). This is due to the fact that, during the absorption of the incident ω_{L1} photon, the number N of ω_{L2} photons does not change, so that the total system cannot go, by an interaction with the ω_{L1} photon, from $|g_1, (N)_2\rangle$ to $|\varphi_2\rangle = |g_2, (N+1)_2\rangle$. Furthermore, the dipole moment operator appearing in the interaction hamiltonian V has no matrix element between g_1 and g_2 . It is only because the dressed state $|\varphi_2\rangle$ contains a small admixture of $|\varphi_e\rangle = |e, (N)_2\rangle$ (see Eq. (4.11b)), that the system can go from $|g_1, (N)_2\rangle$ to $|\varphi_2\rangle$ when $\Omega_2 \neq 0$. Such a contamination can be described in terms of virtual absorptions and emissions of ω_{L2} photons by the atom in g_2 . So, we expect that the scattering path passing through $|\varphi_2\rangle$ could be described in the basis of bare states provided that we introduce, in addition to the ω_{L1} and ω photons which are the only ones to appear in figures 3 and 4, extra ω_{L2} photons to describe such contamination effects.

To carry out such a program, we come back to equation (4.13), and we calculate each term of the bracket, at the lowest order in Ω_2 where it is not vanishing. The first term, which corresponds to the path remaining open when $\Omega_2 = 0$, can be calculated to order zero in Ω_2 .

We then have $\alpha \simeq \langle \varphi_e | \varphi_e \rangle \simeq 1$, $z_1 \sim -i\Gamma/2$, so that :

$$\alpha \langle \varphi_e | \varphi_e \rangle \frac{1}{\delta_1 - z_1} \simeq \frac{1}{\delta_1 + i\frac{\Gamma}{2}} \tag{4.14}$$

The second term requires more caution. Both β and $\langle \varphi_e | \varphi_2 \rangle$ vanish when $\Omega_2 = 0$. They appear only to first order in Ω_2 and, at this order, one gets from (4.11) :

$$\beta \simeq \langle \varphi_e | \varphi_2 \rangle \simeq \frac{\Omega_2/2}{\delta_2 + i\frac{\Gamma}{2}} \tag{4.15}$$

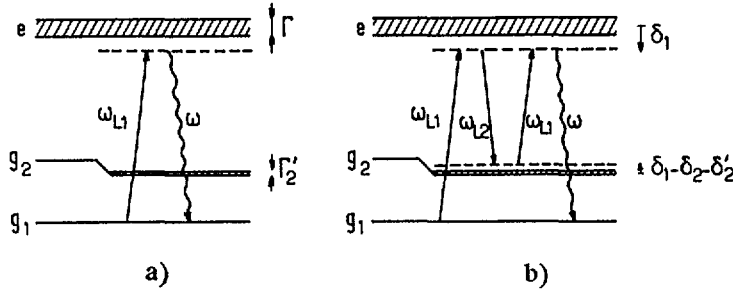


Fig. 5. — Diagrammatic representation of the scattering process in terms of bare states including the light shifts and radiative broadenings due to the ω_{L2} photons. a) Rayleigh scattering process from g_1 (absorption of ω_{L1} , followed by the spontaneous emission of ω). b) Stimulated Raman process bringing the atom from g_1 to g_2 (absorption of ω_{L1} and stimulated emission of ω_{L2}) followed by a spontaneous Raman process bringing the atom from g_2 to g_1 (absorption of ω_{L2} and spontaneous emission of ω).

so that, using (4.2), we can write :

$$\begin{aligned} \beta \langle \varphi_e | \overline{|\varphi_2\rangle} \rangle \frac{1}{\delta_1 - z_{II}} &\simeq \frac{(\Omega_2/2)^2}{(\delta_2 + i\frac{\Gamma}{2})^2} \frac{1}{\delta_1 - \delta_2 - \delta_2' + i\frac{\Gamma}{2}} \\ &\simeq \frac{(\Omega_2/2)^2}{(\delta_1 + i\frac{\Gamma}{2})^2} \frac{1}{\delta_1 - \delta_2 - \delta_2' + i\frac{\Gamma}{2}} \end{aligned} \quad (4.16)$$

In going from the first line of (4.16) to the second line, we have used the fact that, due to the second denominator the whole expression is large only when $\delta_1 \simeq \delta_2 - \delta_2'$, so that we can replace in the first denominator, which gives rise to slow variations (because of the large $i\Gamma/2$ term), δ_2 by $\delta_1 + \delta_2' \simeq \delta_1$. Inserting (4.14) and (4.16) into (4.13), we finally get :

$$T_{\tilde{n}} \simeq T_{\tilde{n}}^I + T_{\tilde{n}}^{II} \quad (4.17)$$

with

$$T_{\tilde{n}}^I \simeq \frac{\hbar\Omega}{2} \frac{1}{\hbar(\delta_1 + i\frac{\Gamma}{2})} \frac{\hbar\Omega_1}{2} \quad (4.18a)$$

$$T_{\tilde{n}}^{II} \simeq \frac{\hbar\Omega}{2} \frac{1}{\hbar(\delta_1 + i\frac{\Gamma}{2})} \frac{\hbar\Omega_2}{2} \frac{1}{\hbar(\delta_1 - \delta_2 - \delta_2' + i\frac{\Gamma}{2})} \frac{\hbar\Omega_2}{2} \frac{1}{\hbar(\delta_1 + i\frac{\Gamma}{2})} \frac{\hbar\Omega_1}{2} \quad (4.18b)$$

We can now give a diagrammatic representation of the amplitudes (4.18a) and (4.18b) in terms of bare states e, g_1, g_2 , keeping however the radiative widths and shifts of these levels (for e , we neglect δ_2' and Γ_2' in comparison with Γ , to be consistent with the approximation made in (4.16)). Reading (4.18a) and (4.18b) from right to left, we associate a photon absorption or emission with each Rabi frequency term $\hbar\Omega_1/2$, $\hbar\Omega_2/2$ or $\hbar\Omega/2$, and an intermediate state with each energy denominator, such an energy denominator giving the energy defect between the energy of the initial state and the energy of the intermediate state.

We first consider (4.18a) (Fig. 5a). Starting from g_1 the atom absorbs the ω_{L1} photon ($\hbar\Omega_1/2$ term) and jumps into e , the energy defect being $\hbar\left(\delta_1 + i\frac{\Gamma}{2}\right)$, and then falls back into g_1 by emission of the fluorescence photon ω ($\hbar\Omega/2$ term). Such a process is nothing but ordinary (near resonant) Rayleigh scattering.

The amplitude (4.18b) corresponds to the four-photon process represented in figure 5b. Here also, the atom starts from g_1 and absorbs the ω_{L1} photon ($\hbar\Omega_1/2$ term) to go into e with an energy defect $\hbar\left(\delta_1 + i\frac{\Gamma}{2}\right)$. But now, from e , the atom jumps into g_2 by stimulated emission of one ω_{L2} photon ($\hbar\Omega_2/2$ term), the new energy defect becoming $\hbar\left(\delta_1 - \delta_2 - \delta'_2 + i\frac{\Gamma'}{2}\right)$. Then, the atom absorbs one photon ω_{L2} ($\hbar\Omega_2/2$ term) to return to e , with the same energy defect $\hbar\left(\delta_1 + i\frac{\Gamma}{2}\right)$ as before, and finally falls back into g_1 by spontaneously emitting the fluorescence photon ω ($\hbar\Omega/2$ term). The amplitude $T_{\text{fi}}^{\text{II}}$ thus describes a sequence of two Raman processes, one stimulated Raman process which brings the atom from g_1 to g_2 , followed by a spontaneous Raman processes, which brings back the atom from g_2 to g_1 [15]. The amplitude of such a combined process becomes very large when the second intermediate state is resonant, i.e. when $\delta_1 = \delta_2 + \delta'_2$. The width of the resonance is the width Γ'_2 of g_2 .

The expression (4.18b) of $T_{\text{fi}}^{\text{II}}$ looks like a perturbative expression taken from a Born expansion of the scattering amplitude. Actually this is not the case. The presence of δ'_2 and Γ'_2 in the second energy denominator results in the fact that (4.18b) is a non-perturbative scattering amplitude. The presence of Ω_2^2 in the numerator of (4.18b) does not imply that $T_{\text{fi}}^{\text{II}}$ is of order 2 in Ω_2 . When $\delta_1 = \delta_2 + \delta'_2$, the second energy denominator of (4.18b) becomes equal to $i\Gamma'_2/2$, which is also proportional to Ω_2^2 , so that $T_{\text{fi}}^{\text{II}}$ is then of order 0 in Ω_2 , and can become on the order of, or even larger than T_{fi}^{I} . It would be also wrong to add to (4.17) amplitudes involving more ω_{L2} photons. Equation (4.17) results from the exact expression (4.13), which already contains a resummation of the perturbation series.

5. Conclusion : Connection with Fano profiles.

In the low saturation limit considered in the previous section, $\Gamma \gg \Gamma'_2$, and the excited state e appears as a continuum, in comparison with the narrow levels g_1 and g_2 . Figures 5a and 5b show that there are two distinct paths for going from the discrete state g_1 to the "continuum" e .

The first path appears in figure 5a. It corresponds simply to the absorption of the photon ω_{L1} which brings directly the atom from g_1 to e . The second path, appearing in Fig. 5b, is a three-photon process going through g_2 . A stimulated Raman process (absorption of ω_{L1} + stimulated emission of ω_{L2}) brings the atom from g_1 to g_2 , and then the absorption of one ω_{L2} photon brings the atom from g_2 into the "continuum" e . This second path, which passes through a narrow discrete state g_2 , interferes with the first one, which is a direct path towards the continuum. Such a situation leads to Fano profiles.

To check this point more carefully, we come back to equation (3.20), and, using (4.2) and (4.3), we rewrite the first line of this equation as :

$$T_{\text{fi}} = \frac{\hbar\Omega_1\Omega}{4\left[\delta_1 + \delta'_2 + i\frac{\Gamma - \Gamma'_2}{2}\right]} \frac{\delta_1 - \delta_2}{\delta_1 - \delta_2 - \delta'_2 + i\frac{\Gamma'_2}{2}} \quad (5.1)$$

Because of the presence of $i\Gamma/2$ in the denominator, the first fraction of (5.1) varies very slowly with δ_1 , in comparison with the second fraction. We now transform the second fraction of (5.1), which is the one giving rise to the rapid variations of T_{fi} around $\delta_1 = \delta_2 + \delta'_2$ by introducing the reduced variables :

$$\varepsilon = \frac{\delta_1 - \delta_2 - \delta'_2}{\Gamma'_2/2} \quad (5.2)$$

$$q = \frac{\delta'_2}{\Gamma'_2/2} = \frac{2\delta'_2}{\Gamma'_2} = \frac{2\delta}{\Gamma} \quad (5.3)$$

This allows one to write $|T_{\hbar}|^2$ as :

$$|T_{\hbar}|^2 = \frac{\hbar^2 \Omega_1^2 \Omega^2}{16 \left[(\delta_1 + \delta'_2)^2 + \frac{(\Gamma - \Gamma'_2)^2}{4} \right]} \frac{(\varepsilon + q)^2}{\varepsilon^2 + 1} \quad (5.4)$$

The second fraction of (5.4) is typical of a Fano profile with parameter q .

We have thus proven that the narrow structure of figure 2 is a Fano profile, and we have identified in figure 5 the two interfering pathways which give rise to such a profile.

Acknowledgements.

We thank G. Grynberg for stimulating discussions.

Cet article est un témoignage de notre admiration pour l'oeuvre scientifique de Pierre Jacquinet et de notre reconnaissance pour le travail qu'il a accompli pour le développement de la Recherche Scientifique en France et dont nous avons tous bénéficié.

References

- [1] ALZETTA G., GOZZINI A., MOI L. and ORRIOLS G., *Nuovo Cim.* **B36** (1976) 5.
- [2] GRAY H.R., WHITLEY R.M. and STROUD C.R. Jr, *Opt. Lett.* **3** (1978) 218.
- [3] ARIMONDO E. and ORRIOLS G., *Nuovo Cim. Lett.* **17** (1976) 133.
- [4] RADMORE P.M. and KNIGHT P.L., *J. Phys.* **B14** (1981) 573.
- [5] JANIK G., NAGOURNEY W., DEHMELT H., *J.O.S.A.* **B2** (1985) 1251.
- [6] DALIBARD J., REYNAUD S., COHEN-TANNOUDJI C., in *Interaction of Radiation with Matter*, a Volume in honour of A. Gozzini, Scuola Normale Superiore, Pisa (1987).
- [7] THOMAS J.E., HEMMER P.R., EZEKIEL S., LEIBY C.C., PICARD R.H., WILLIS C.R., *Phys. Rev. Lett.* **48** (1982) 867.
- [8] ASPECT A., ARIMONDO E., KAISER R., VANSTEENKISTE N. and COHEN-TANNOUDJI C., *Phys. Rev. Lett.* **61** (1988) 826 ; *J.O.S.A.* **B6** (1989) 2112.
- [9] GAUBATZ U., RUDECKI P., SCHIEMANN S. and BERGMANN K., *J. Chem. Phys.* **92** (1990) 5363.
- [10] IMAMOGLU A., FIELD J.E., HARRIS S.E., *Phys. Rev. Lett.* **66** (1991) 1154.
- [11] FANO U., *Phys. Rev.* **124** (1961) 1866.
- [12] ARMSTRONG L. Jr., BEERS B.L. and FENEUILLE S., *Phys. Rev. A* **12** (1975) 1903.
- [13] KNIGHT P.L., *Comments At. Mol. Phys.* **15** (1984) 193.
- [14] COHEN-TANNOUDJI C., DUPONT-ROC J. and GRYNBERG G., *Processus d'Interaction entre Photons et Atomes* (Interditions et Editions du CNRS, Paris, 1988). English translation : *Atom-Photon Interactions. Basic Processes and Applications* (Wiley, New-York, 1992).
- [15] Other examples of interferences between different pathways, one of them involving a stimulated Raman process may be found in : GRYNBERG G. and BERMAN P.R., *Phys. Rev.* **A41** (1990) 2677. In the problem considered in this paper, the dissipative process is not spontaneous emission, but collisions.